

Small-angle elastic p - p scattering at 30, 50, and 70 GeV

I. M. Geshkov, N. L. Ikov, P. K. Markov, and R. K. Trayanov

Institute of Nuclear Research and Nuclear Energy, Sofia, Bulgaria

(Received 19 February 1974)

A thin polyethylene target was exposed to the internal proton beam of the Serpukhov accelerator at 30, 50, and 70 GeV. The wide-angle recoil protons were registered by photoemulsion stacks and the differential cross sections of the elastic p - p scattering in the range of four-momentum transfer squared $0.0025 \leq |t| \leq 0.12$ (GeV/c)² were measured. The ratio of the real to the imaginary part of the forward nuclear amplitude α , the slope parameter of the diffraction peak b , and the total elastic cross section σ_{el} were found to be as follows: at 30 GeV, $\alpha = -0.183 \pm 0.051$, $b = 10.61 \pm 0.27$ (GeV/c)⁻², $\sigma_{el} = 7.7 \pm 0.2$ mb; at 50 GeV, $\alpha = -0.068 \pm 0.040$, $b = 11.25 \pm 0.28$ (GeV/c)⁻², $\sigma_{el} = 7.0 \pm 0.2$ mb; at 70 GeV, $\alpha = -0.104 \pm 0.065$, $b = 11.21 \pm 0.40$ (GeV/c)⁻², $\sigma_{el} = 7.1 \pm 0.2$ mb.

I. INTRODUCTION

During the last ten years many experiments have been performed to study small-angle elastic p - p scattering at the high-energy accelerators. The differential cross sections in the range of four-momentum transfer squared $|t| < 0.2$ (GeV/c)² give information about the slope of the diffraction peak (b), as well as the ratio of the real to the imaginary part of the forward elastic p - p nuclear amplitude (α). The smallest $|t|$ value accessible for measurement of the differential cross section is an important feature of these experiments. In the region of $|t| \approx 0.003$ (GeV/c)² the nuclear and Coulomb amplitudes are comparable. Measuring the differential cross sections in this region one can observe the interference between both amplitudes and one can therefore determine the magnitude and the sign of α .

Various kinds of magnetic spectrometers were used for investigations with external proton beams¹⁻³ and with the colliding beams at CERN.⁴⁻⁶ For the case of internal proton beams a method was developed for detecting the wide-angle recoil protons scattered from an internal thin polyethylene target.⁷⁻⁹ Recently a substantial improvement of this method was made. A hydrogen or deuteron gas-jet internal target and silicon solid-state detectors were used on-line with a computer at the Serpukhov^{10,11} and Batavia^{12,13} accelerators.

The knowledge of the energy dependence of b and α up to the highest available energies is of great importance. The experimental data can be compared to the predictions of the dispersion-relation theory, the Regge-pole model, the quasipotential approach, and some other models of the strong-interaction behavior at high energies.

In this paper we report our results on the measurements of the differential cross sections of

elastic p - p scattering at 30, 50, and 70 GeV in the range of four-momentum transfer squared $0.0025 < |t| < 0.12$ (GeV/c)². In addition, the results for the ratio of the real to the imaginary part of the forward nuclear amplitude, the slope parameter of the diffraction peak, and the total elastic p - p cross section at these energies are given.

II. EXPERIMENTAL METHOD

The layout of the experiment is shown in Fig. 1. An internal thin polyethylene target (T) was used in one of the linear sections of the Serpukhov accelerator. It was 10 mm wide (along the proton beam), 20 mm long, and about 1 μ m thick, and was supported by 7- μ m-thick glass fibers. The secondary particles, including the recoil protons from the elastic p - p scattering coming out from the target in the laboratory angle range 79° - 90° , were registered by four photoemulsion stacks (A, B, C, D). They were 3.59 m away from the target in an evacuated channel. Three scintillation counters (M) were used to choose the appropriate conditions of the exposure and to monitor the incident proton beam.

The small thickness of the target was chosen in order to decrease the multiple Coulomb scattering of the recoil protons and their energy losses in the target. Due to the small target mass (about 10^{-4} g) the incident proton beam could pass through it several thousand times. Because of that, only a few cycles of the accelerator were enough for a suitable exposure.

Stack A consisted of only one 200- μ m-thick photoemulsion pellicle with a surface of 10×20 cm². In order to increase the precision of range measurements the pellicle was a diluted emulsion, which after the processing had a shrinking coef-

ficient of about $k=0.7$. The stack had such a position that it registered the secondary particles scattered in the laboratory angle range 87° – 90° . They entered into the stack perpendicularly to the pellicle surface. The recoil protons from the elastic p - p scattering in this angle region have ranges less than $150\ \mu\text{m}$, and they all stop in the emulsion pellicle. To determine the differential cross section at a given laboratory angle a thin strip on the emulsion surface, 2 mm wide and 5 or 10 mm long, was scanned twice by microscope with an optical magnification of 8×60 . All particles stopping in the emulsion were registered and their ranges were measured. In the range distribution of the particles there is a well-pronounced peak corresponding to the wide-angle recoil protons from the elastic p - p scattering. The number of particles in the peak after the subtraction of the background is considered as the number of the elastic events. The so-called combined background was determined using the ranges outside the peaks, as well as the ranges measured in strips, where particles scattered from the target at laboratory angles greater than 90° were registered and no elastic recoil protons were present.

Stack *B* consisted of a few $600\text{-}\mu\text{m}$ standard emulsion pellicles of type NIKFI BR-I with a surface of $10\times 15\ \text{cm}^2$. The particles coming out from the target in the laboratory angle region 85.0° – 86.5° were registered. They entered stack *B* perpendicular to the pellicle surface. In this angle region the recoil protons have ranges less than $1000\ \mu\text{m}$; thus only the two top layers of the stack were used for scanning and measuring the ranges of the stopping particles.

Stacks *C* and *D* consisted of about 30 standard photoemulsion pellicles with a surface of 5×15

cm^2 and a thickness of $600\ \mu\text{m}$. The secondary particles entered the stacks parallel to the emulsion surface. They registered the particles scattered from the target in the laboratory angle regions 82.0° – 83.7° and 79.2° – 81.0° , respectively. To determine the differential cross section at a given laboratory angle the scanning was performed on a thin strip $2\times 10\ \text{mm}^2$ along the particle ranges and centered at the end of the recoil protons. All secondary particles stopping in this strip were registered and their ranges were measured.

About 20 differential cross sections were measured for each of the incident proton energies (8–9 cross sections in stack *A*, 4–5 in stack *B*, 4 in stack *C*, and 4 in stack *D*). The range distributions of the particles, as well as the background for some of the peaks at 30 GeV incident proton energy, are shown in Figs. 2 and 3. Similar distributions were obtained for 50- and 70-GeV incident proton energies.

The background particles are due mostly to the evaporation of the carbon nuclei of the target and to the quasielastic scattering in these nuclei.

The widths of the peaks observed are due mainly to the following reasons: (1) the incident proton angle distribution, (2) the fact that the target is not pointlike, (3) the multiple scattering of the recoil protons in the target, and (4) the measurement errors and the straggling in the emulsion. For the peaks of the recoil protons with ranges less than $1000\ \mu\text{m}$ the main reason is the third one.

The angle and momentum resolution of the experiment were about 3 mrad and $3\ \text{MeV}/c$, respectively. Because of this high resolution the contribution of the quasielastic p - p scattering in the carbon nuclei was estimated to be about 2%,

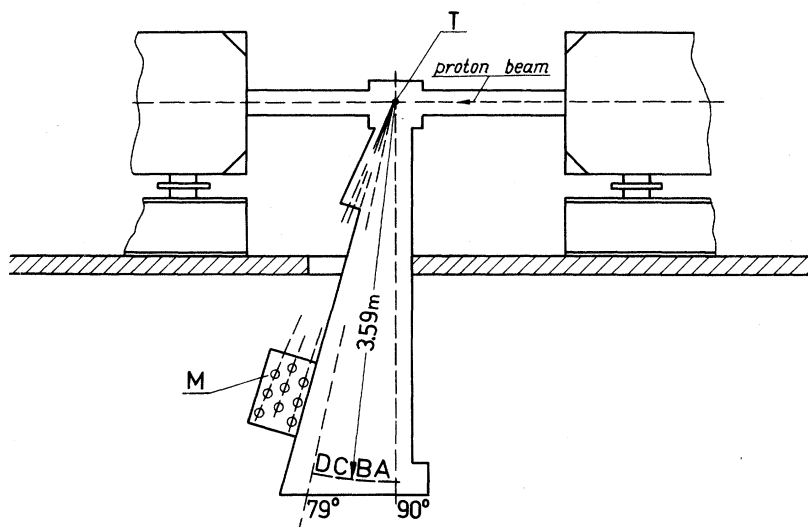


FIG. 1. Simplified layout of the experimental arrangement.

which is less than the statistical error of our experiment.

The double-scanning efficiency for the long ranges was very high. A correction of the elastic-event number was done only for recoil proton ranges less than $100 \mu\text{m}$. It was 12% for ranges of $R = 30 \mu\text{m}$, 5% for $R = 40 \mu\text{m}$, and 2% for $R = 60 \mu\text{m}$.

The ratio (r) of the elastic events to the background particles depends on the wide-angle recoil proton ranges. For instance, at 30 GeV it changes for stack A from $r = 0.7$ to $r = 1.4$, for stack B from $r = 3.6$ to $r = 7.9$, for stack C from $r = 8.4$ to $r = 9.4$, and for stack D from $r = 6.4$ to $r = 6.7$.

III. EXPERIMENTAL RESULTS

The numbers of all secondary particles registered and measured and those of elastic events found for each of the incident proton energies are given in Table I. The statistics of the elastic events in stack A were increased about 50% compared to our preliminary results published earlier.¹⁴

The experimental data for the differential cross sections in relative units were fitted to the well-

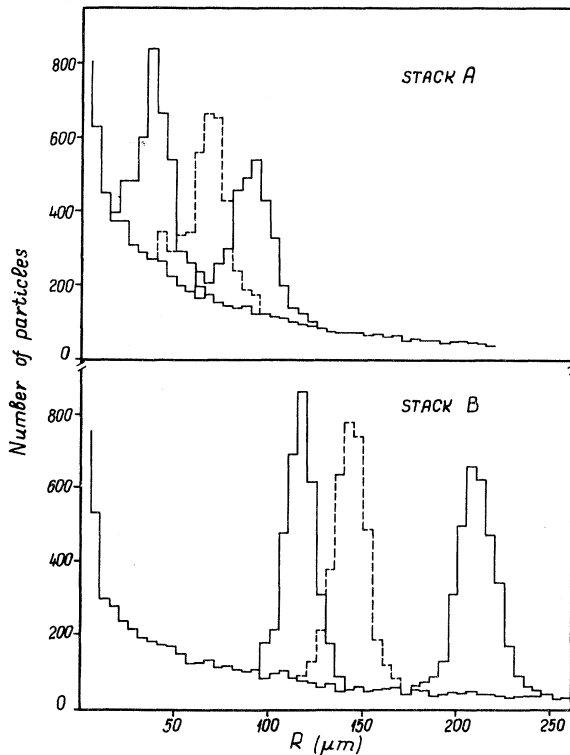


FIG. 2. Range distributions of some peaks at 30 GeV in stacks A and B, corresponding to $t = -0.0036, -0.0049, -0.0060, -0.0131, -0.0148, \text{ and } -0.0179 \text{ (GeV}/c)^2$.

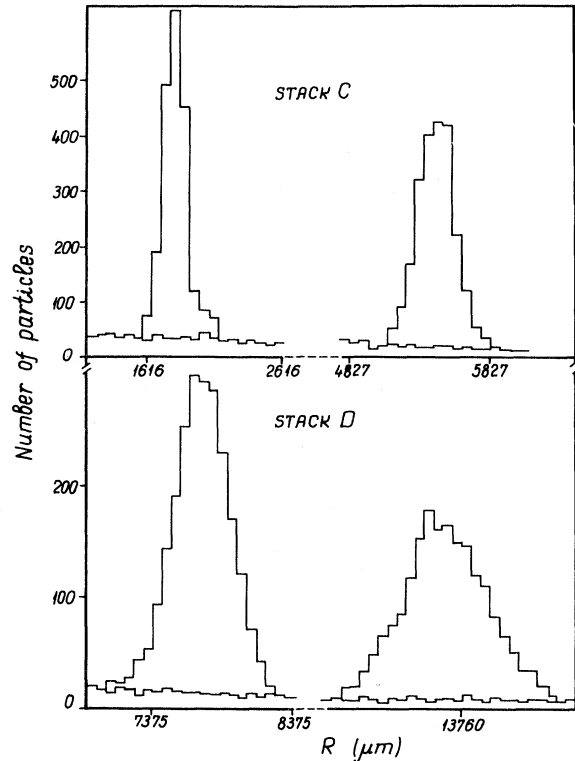


FIG. 3. Range distributions of some peaks at 30 GeV in stacks C and D, corresponding to $t = -0.0413, -0.0648, -0.0873, \text{ and } -0.1189 \text{ (GeV}/c)^2$.

known expression

$$\frac{d\sigma}{d|t|} = C \left[(1 + \alpha^2) A_I^2(t) + A_C^2(t) - 2A_I(t)A_C(t)(\alpha + 2\delta) \right], \quad (1)$$

where C is a normalization parameter, $\alpha = A_R(0)/A_I(0)$ is the ratio of the real to the imaginary part of the forward nuclear amplitude, $A_I(t) = (\sigma_{\text{tot}}^2/16\pi\hbar^2)\exp(\frac{1}{2}bt)$ is the imaginary part of the nuclear amplitude, $A_C(t) = (2e^2\sqrt{\pi}/\beta c|t|) \times F_C(t)$ is the Coulomb amplitude and

$$F_C(t) = G_E^2 \left(1 - \frac{\mu^2 t}{4M^2} \right) / \left(1 - \frac{t}{4M^2} \right)$$

TABLE I. Numbers N_1 of the differential cross sections measured, N_2 of the elastic events found, and N_3 of the secondary particles registered, at each of the incident proton energies.

E (GeV)	N_1	N_2	N_3
30	21	34 545	93 587
50	23	33 240	95 324
70	21	20 696	68 318

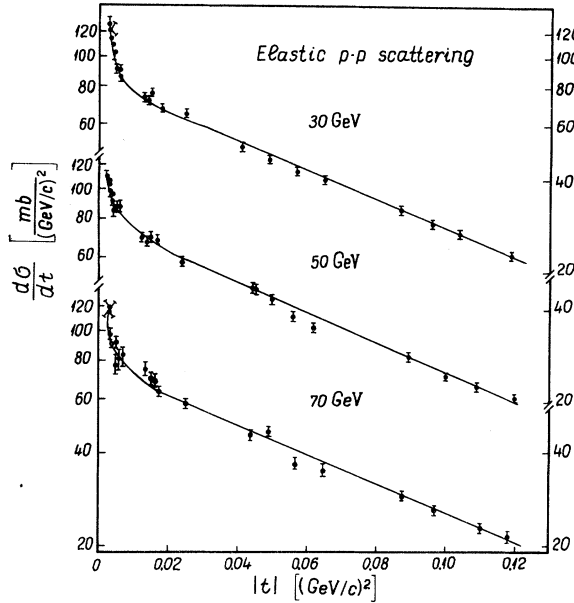


FIG. 4. The differential cross sections of the elastic p - p scattering at 30, 50, 70 GeV. The solid lines are the fits of Eq. (1) with $C = 1$.

is the proton electromagnetic form factor, with¹⁵ $G_E = 1 + 2.77t$. The phase between the Coulomb and the nuclear amplitude is given by¹⁶

$$2\delta = \frac{1}{137\beta} \ln\left(\frac{1.06t}{\alpha}\right)^2$$

(the value of a is taken from Ref. 17).

The differential cross sections normalized to the optical point are shown in Fig. 4. The curves are the fits from Eq. (1). The normalization parameter C , the ratio α of the real to the imaginary part of the forward nuclear amplitude, and the slope parameter b of the diffraction peak are given in Table II. There are also shown the χ^2 values per one degree of freedom. The results

TABLE II. Ratio (α) of the real to the imaginary part of the forward nuclear amplitude and the slope of the diffraction peak (b) of the p - p elastic scattering at 30, 50, and 70 GeV.

E (GeV)	C	$-\alpha$	b [(GeV/c) ⁻²]	χ^2 /D.F.
30 I	0.846 ± 0.033	0.183 ± 0.051	10.61 ± 0.27	20.9/18
II	0.847 ± 0.016	0.181 ± 0.033	10.62 fixed	20.9/19
III	0.947 ± 0.010	0 fixed	11.48 ± 0.18	40.0/19
50 I	1.013 ± 0.027	0.068 ± 0.040	11.25 ± 0.28	32.6/20
II	0.999 ± 0.014	0.085 ± 0.028	11.09 fixed	32.9/21
III	1.055 ± 0.011	0 fixed	11.53 ± 0.19	24.8/21
70 I	1.008 ± 0.043	0.104 ± 0.065	11.21 ± 0.40	27.4/18
II	1.025 ± 0.020	0.081 ± 0.042	11.40 fixed	27.6/19
III	1.066 ± 0.016	0 fixed	11.72 ± 0.27	30.4/19

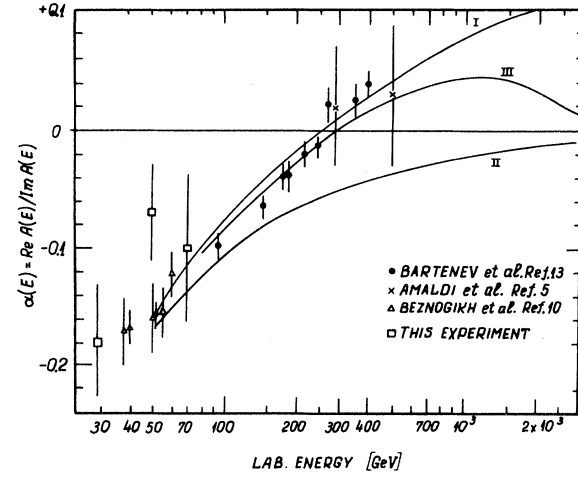


FIG. 5. The ratio α of the real to the imaginary part of the forward p - p nuclear amplitude as a function of the energy. The curves are dispersion-relation calculations (Ref. 13) assuming that (i) $\sigma_t(p\bar{p})$ and $\sigma_t(\bar{p}p)$ increase as $\ln^2(s/122)$, (ii) $\sigma_t(p\bar{p})$ is constant for $E > 120$ GeV at 38 mb, (iii) $\sigma_t(p\bar{p})$ becomes constant above 2000 GeV at 43.5 mb. In each case it is assumed that $\sigma_t(\bar{p}p)$ approaches $\sigma_t(p\bar{p})$ as $E^{-0.002}$.

for two other cases, where b or α were taken as fixed parameters, are given too.

The data obtained for α along with data of other experiments are plotted in Fig. 5 against the incident proton energy. Our results are in agreement within the error limits with the corresponding energy points of the other experiments. The dispersion-relation prediction for α assuming an increase in the p - p total cross section at least up to 2000 GeV is consistent with the experimental data up to 500 GeV.¹³

Our data for b along with other data are plotted

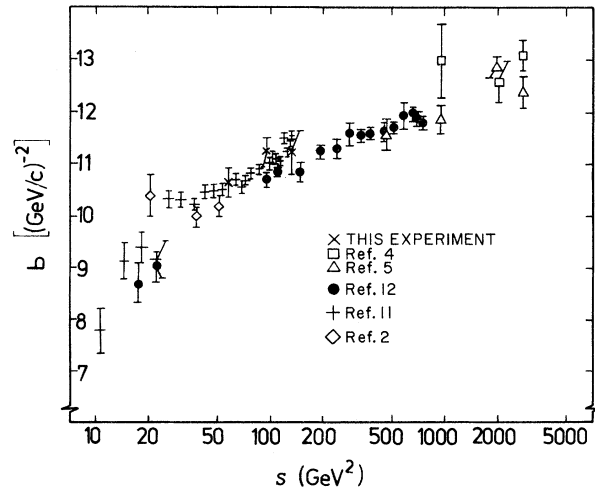


FIG. 6. Slope of the diffraction peak of the elastic p - p scattering as a function of the square of the c.m. energy.

in Fig. 6 against the square of the c.m. energy (s). The results obtained for b at 30, 50, and 70 GeV are in agreement with the data of other experiments. The parameter b is increasing with s . According to the optical model the radius of the p - p interaction is related to b , $R = 2\hbar\sqrt{b}$; therefore the radius increases with energy too. The energy dependence of b for $s > 100$ GeV² can be parametrized with the expression

$$b(s) = b_0 + 2\alpha' \ln(s/s_0) \quad (2)$$

following from the one-Regge-pole model, where α' is the slope of the Pomeron trajectory. The fit of the experimental data¹² to Eq. (2) gives $b_0 = 8.23 \pm 0.27$ (GeV/c)⁻² and $\alpha' = 0.278 \pm 0.024$ (GeV/c)⁻².

The total elastic cross sections were determined using the formula

$$\sigma_{el} = (1 + \alpha^2) \frac{\sigma_{tot}^2}{16\pi\hbar^2} \left[\int_0^{0.12} \exp(bt) d|t| + \int_{0.12}^{0.81} \exp(bt + ct^2) d|t| \right], \quad (3)$$

where¹⁸ $c = 2.5$ (GeV/c)⁻⁴. They turned out to be 7.7 ± 0.2 mb at 30 GeV, 7.0 ± 0.2 mb at 50 GeV, and 7.1 ± 0.2 mb at 70 GeV.

ACKNOWLEDGMENTS

We are very grateful to Professor A. A. Logunov and Professor R. M. Sulyaev for their kind permission to carry out the experiment at the Serpukhov accelerator. Acknowledgments are due to Dr. V. A. Nikitin, Dr. V. A. Sviridov, Dr. L. S. Zolin, and Dr. M. G. Shafranov for their help and valuable discussions, to S. I. Lyobomilov for the processing of the emulsion stacks, and to our group of scanners.

¹K. J. Foley, R. S. Gilmore, R. S. Jones, S. J. Lindenbaum, W. A. Love, S. Ozaki, E. H. Willen, R. Yamada, and L. C. L. Yuan, *Phys. Rev. Lett.* **14**, 74 (1965).

²G. Bellittini, G. Cocconi, A. N. Diddens, E. Lillethun, J. P. Scanlon, and A. M. Wetherell, *Phys. Lett.* **19**, 705 (1966).

³A. E. Taylor, A. Ashmore, W. S. Chapman, D. F. Falla, W. H. Range, D. B. Scott, A. Astbury, F. Capocci, and T. G. Walker, *Phys. Lett.* **14**, 54 (1965).

⁴U. Amaldi, R. Biancastelli, G. Bosio, G. Matthiae, J. V. Allaby, W. Bartel, G. Cocconi, A. N. Diddens, R. W. Dobinson, V. Elings, J. Litt, L. S. Rochester, and A. M. Wetherell, *Phys. Lett.* **36B**, 504 (1971).

⁵U. Amaldi, R. Biancastelli, C. Bosio, G. Matthiae, J. V. Allaby, W. Bartel, M. M. Block, G. Cocconi, A. N. Diddens, R. W. Dobinson, J. Litt, and A. M. Wetherell, *Phys. Lett.* **43B**, 231 (1973).

⁶G. Barbiellini, M. Bozzo, P. Dariulat, G. Diambrini Palazzi, G. De Zorzi, A. Fainberg, M. I. Ferrero, M. Holder, A. McFarland, G. Maderni, S. Orito, J. Pilcher, C. Rubbia, A. Santroni, G. Sette, A. Standa, P. Strolin, and K. Tittel, *Phys. Lett.* **39B**, 663 (1972).

⁷V. A. Nikitin, A. A. Nomofilov, V. A. Sviridov, L. N. Strunov, and M. G. Shafranov, *Prib. Tek. Eksp.* **6**, 18 (1963).

⁸L. F. Kirillova, V. A. Nikitin, V. S. Pantuev, V. A. Sviridov, L. N. Strunov, M. N. Khachatryan, L. G. Khristov, M. G. Shafranov, Z. Korbil, L. Rob, S. Damyanov, A. Zlateva, Z. Zlatanov, V. Iordanov, Kh. Kanazirski, P. Markov, T. Todorov, Kh. Chernev, N. Dalkhazhav, and T. Tuvdendorzh, *Yad. Fiz.* **1**, 533 (1965) [*Sov. J. Nucl. Phys.* **1**, 379 (1965)].

⁹N. Dalkhazhav, P. A. Devinski, V. Zayachki, Z. Zlatanov, L. S. Zolin, L. F. Kirillova, Z. Korbil, P. K. Markov, Ngo Kuang Zui, Nguen Din ti, V. A. Nikitin, L. Rob, V. A. Sviridov, D. Tuvdendorzh, L. G. Khristov, Kh. Chernev, Truong Bien, and M. G. Shafranov, *Yad. Fiz.* **8**, 342 (1968) [*Sov. J. Nucl. Phys.* **8**, 196 (1968)].

¹⁰G. G. Beznogikh, A. Bujak, L. F. Kirillova, B. A. Morozov, V. A. Nikitin, P. V. Nomokonov, A. Sandacz, M. G. Shafranov, V. A. Sviridov, Truong Bien, V. I. Zayachki, N. K. Zhidkov, and L. S. Zolin, *Phys. Lett.* **39B**, 411 (1972).

¹¹G. G. Beznogikh, A. Bujak, V. A. Nikitin, M. G. Shafranov, V. A. Sviridov, Truong Bien, L. V. Vikhlyantseva, V. I. Zayachki, and L. S. Zolin, *Phys. Lett.* **43B**, 85 (1973).

¹²V. Bartenev, A. Kuznetsov, B. Morozov, V. Nikitin, Y. Pilipenko, V. Popov, L. Zolin, R. A. V. Carrigan, Jr., E. Malamud, R. Yamada, R. L. Cool, K. Goulianos, I-Hung Chiang, A. C. Melissinos, D. Gross, and S. L. Olsen, *Phys. Rev. Lett.* **29**, 1755 (1972); **31**, 1088 (1973).

¹³V. Bartenev, R. A. Carrigan, Jr., I-Hung Chiang, R. L. Cool, K. Goulianos, D. Gross, A. Kuznetsov, E. Malamud, A. C. Melissinos, B. Morozov, V. Nikitin, S. L. Olsen, Y. Pilipenko, V. Popov, R. Yamada, and L. Zolin, *Phys. Rev. Lett.* **31**, 1367 (1973).

¹⁴Kh. M. Chernev, I. M. Geshkov, N. L. Ikov, P. K. Markov, and V. I. Zayachki, *Phys. Lett.* **36B**, 266 (1971).

¹⁵L. N. Hand, D. G. Miller, and Richard Wilson, *Rev. Mod. Phys.* **35**, 335 (1963).

¹⁶H. A. Bethe, *Ann. Phys. (N.Y.)* **3**, 190 (1958).

¹⁷G. Bialkowski and S. Pokorski, *Nuovo Cimento* **57A**, 219 (1968).

¹⁸G. G. Beznogikh, A. Bujak, V. A. Nikitin, M. G. Shafranov, V. A. Sviridov, Truong Bien, L. V. Vikhlyantseva, V. I. Zayachki, and L. S. Zolin, JINR Report No. E1-6743, 1972 (unpublished).